


IMAGES OF SPINE CARE

Pelvic Ewing sarcoma: a radiologic and histopathologic correlation

An otherwise healthy 22-year-old service member developed an insidious onset of new right-sided sacroiliac (SI) joint and radicular pain of the lower extremity while deployed abroad. Upon return to the United States, the patient noted 40 lb of unintentional weight loss and progressive swelling of the right lower extremity. Initial radiographs displayed a pelvic lytic lesion with SI joint erosion (Fig. 1). Computed tomography further demonstrated the destructive SI joint mass (Fig. 2). Magnetic resonance imaging displayed a large heterogeneously enhancing soft tissue mass with areas of soft tissue necrosis (Fig. 3). A computed tomography biopsy re-

turned CD99 and FLI-1 positive, and negative for pan-keratin, CD56, synaptophysin, CD45, leukocyte common antigen, CD3, and CD20. Fluorescent in situ hybridization was positive for EWSR1 rearrangement.

After completion of neoadjuvant chemotherapy (vincristine sulfate, cyclophosphamide, topotecan hydrochloride), the patient underwent right hemipelvectomy with partial sacrectomy (95% tumor necrosis noted). Microscopic sections revealed findings that were consistent with post-neoadjuvant Ewing sarcoma, with some perivascular sparing (Fig. 4). The patient has successfully completed adjuvant chemotherapy and is scheduled for interval pelvic reconstruction. As typical in patients presenting with Ewing sarcoma after the second decade of life, the patient's initial symptoms were insidious harbingers of a pelvic mass [1–3].

References

- [1] Ozaki T. Diagnosis and treatment of Ewing sarcoma of the bone: a review article. *J Orthop Sci* 2015;20:250–63.
- [2] Maheshwari AV, Cheng EY. Ewing sarcoma family of tumors. *J Am Acad Orthop Surg* 2010;18:94–107.
- [3] Walczak BE, Irwin RB. Sarcoma chemotherapy. *J Am Acad Orthop Surg* 2013;21:480–91.



Fig. 1. Initial plain radiographs demonstrating lucency about the inferior aspect of the right posterior ilium with sacroiliac joint destruction (Top: antero-posterior pelvis view; Bottom: right obturator oblique view).

Bryan K. Lawson, MD^a
 Harold J. Goldstein, MD^a
 Richard K. Hurley, MD^a
 Robert L. Hutton, MD^b
 Edward R. Anderson III, MD^a
 Joseph F. Alderete, MD^a

^aDepartment of Orthopedic Surgery
 San Antonio Military Medical Center
 3551 Roger Brooke Drive

San Antonio, TX 78234, USA

^bDepartment of Pathology
 San Antonio Military Medical Center
 3551 Roger Brooke Drive

San Antonio, TX 78234, USA

FDA device/drug status: Not applicable.

Author disclosures: **BKL:** Nothing to disclose. **HJG:** Nothing to disclose. **RKH:** Nothing to disclose. **RLH:** Nothing to disclose. **ERA:** Nothing to disclose. **JFA:** Nothing to disclose.

Conflicts of interest and Source of funding: No financial or other conflicts of interest are declared by the authors.

The view(s) expressed herein are those of the author(s) and do not reflect the official policy or position of Brooke Army Medical Center, the US Army Medical Department, the US Army Office of the Surgeon General, the Department of the Army, the Department of the Air Force and Department of Defense, or the US Government.

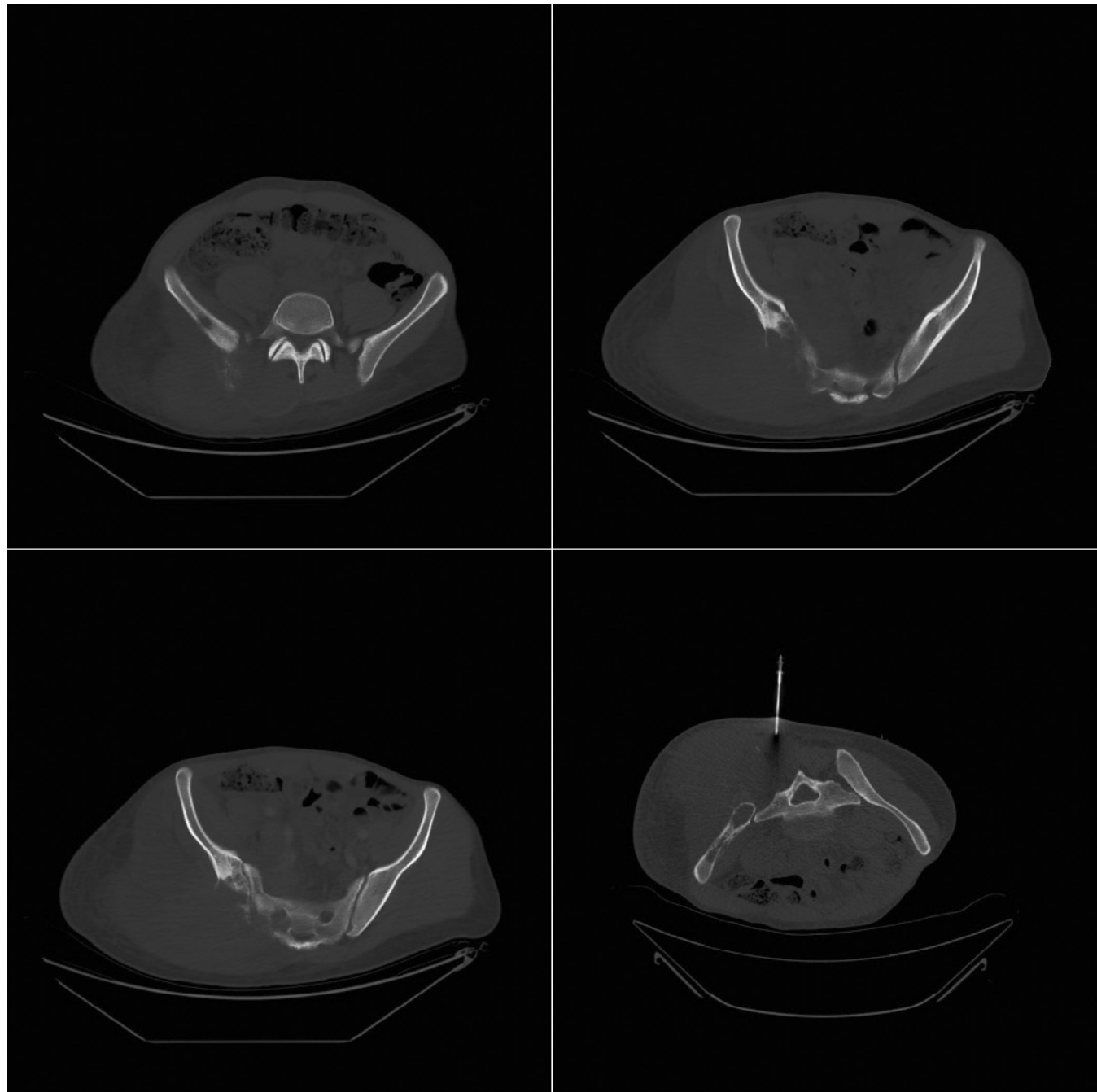


Fig. 2. Initial computed tomography (CT) scan and CT biopsy revealing the extent of osseous erosion secondary to the right-sided pelvic mass with soft tissue extension.

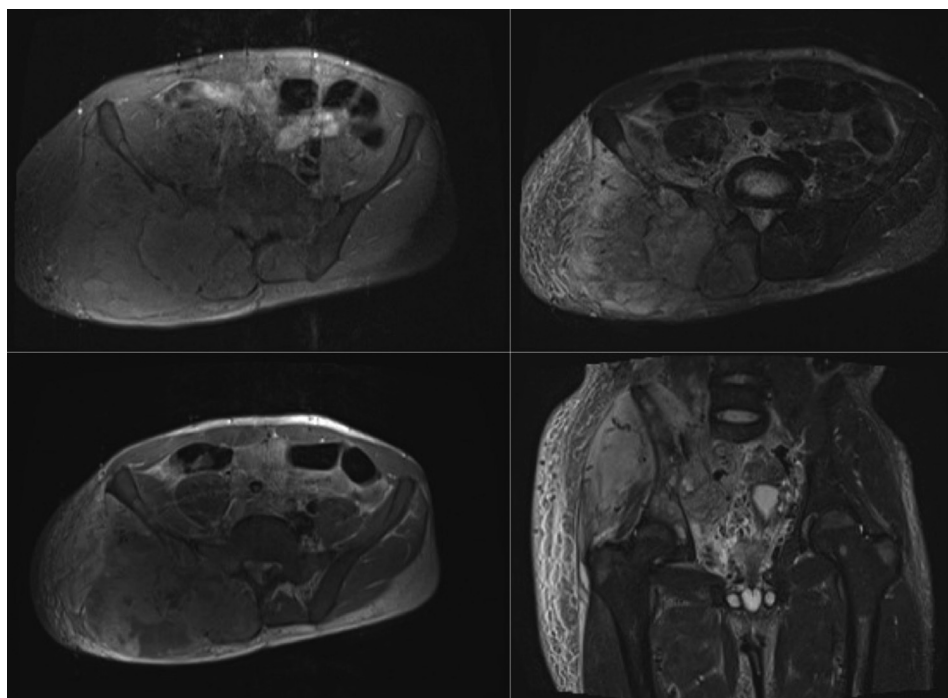


Fig. 3. Magnetic resonance imaging demonstrating the degree of pelvic soft tissue extension (Top left: axial T1 sequence; Top right: axial short tau inversion recovery [STIR] sequence; Bottom left: axial T1 post-contrast sequence; Bottom right: STIR sequence).

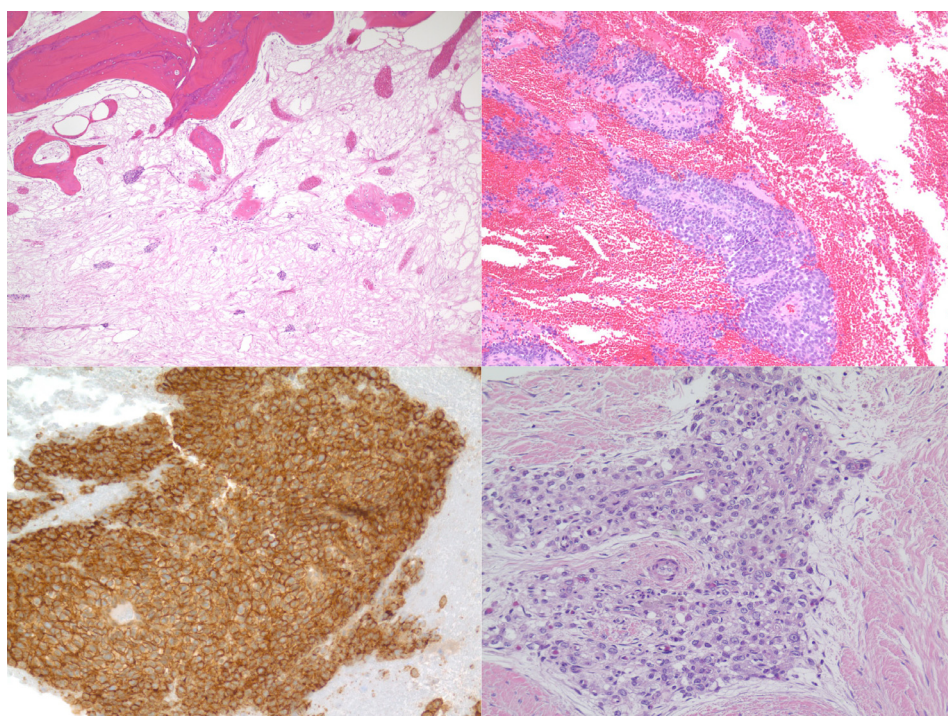


Fig. 4. Top left: Hematoxylin-eosin (magnification $\times 4$) resection specimen showing only scattered tumor cell clusters within hyalinized stroma indicating a high percentage of tumor cell necrosis. Top right: Hematoxylin-eosin (magnification $\times 10$) section of resection specimen revealing perivascular sparing of tumor necrosis. Although the vast majority of tumor was necrotic, viable tumor cells were most easily observed adjacent to small capillaries and venules. Bottom left: CD99 stain (magnification $\times 20$) section demonstrating classic membrane accentuation characteristic of Ewing sarcoma. Bottom right: Hematoxylin-eosin (magnification $\times 20$) tumor cell cluster in soft tissue with notable post-chemotherapy changes to include nuclear enlargement with prominent nucleoli, nests, and solid sheets of small round blue cells with occasional primitive rosette formations, angulated hyperchromatic nuclei, and bubbly eosinophilic glycogen-rich cytoplasm.